



NMRF/TR/04/2021



सत्यमेव जयते

TECHNICAL REPORT

**An operational lightning verification system for the
evaluation of NCMRWF regional Unified Model**

Saji Mohandas and A. Jayakumar

October 2021

**National Centre for Medium Range Weather Forecasting
Ministry of Earth Sciences, Government of India
A-50, Sector-62, NOIDA-201309, INDIA**

An operational lightning verification system for the evaluation of NCMRWF regional Unified Model

Saji Mohandas and A. Jayakumar

NCMRWF Technical Report No: NMRF/TR/04/2021

October 2021

National Centre for Medium Range Weather Forecasting

Ministry of Earth Sciences, Government of India

A-50, Sector 62, NOIDA-201 309, India

Abstract

From October, 2020, the lightning forecasts from National Centre for Medium Range Weather Forecasting (NCMRWF) operational limited area model at 4km resolution (NCUM-R) are being routinely compared against the Earth Network Lightning Sensor (ENLS) datasets from two independent sources of data; Indian Air Force (IAF) and Indian Institute of Tropical Meteorology (IITM). An algorithm was developed for merging the two independent sources of datasets to avoid possible duplication of the flash counts and the results of the model verification for the current and previous versions are discussed in the current report. The evaluation of the latest Regional Atmosphere version 2 for tropics (RA2T) against the previous version (RA1T) was conducted using IAF/IITM lightning observations as well as 25km resolution satellite-gauge merged rainfall analysis. Later ocean masking was done for the lightning data as the observations were found to have less coverage over the vast oceanic areas surrounding the Indian peninsula. The comparison of gridded statistics for Indian domain covering entire India, but considering land only grid points was operationalised from 1 October, 2021. Comparison of the current masked extended Indian domain (IN) against the previous All India (AI) box also was carried out and presented in the current report.

1	Name of the Institute	National Centre for Medium Range Weather Forecasting
2	Document Number	NMRF/TR/04/2021
3	Date of publication	October 2021
4	Title of the document	An operational lightning verification system for the evaluation of NCMRWF regional Unified Model
5	Type of Document	Technical Report
6	No. of pages & Figures	24 & 18
7	Number of References	32
8	Author (s)	Saji Mohandas and A. Jayakumar
9	Originating Unit	NCMRWF
10	Abstract	<p>From October, 2020, the lightning forecasts from National Centre for Medium Range Weather Forecasting (NCMRWF) operational limited area model at 4km resolution (NCUM-R) are being routinely compared against the Earth Network Lightning Sensor (ENLS) datasets from two independent sources of data; Indian Air Force (IAF) and Indian Institute of Tropical Meteorology (IITM). An algorithm was developed for merging the two independent sources of datasets to avoid possible duplication of the flash counts and the results of the model verification for the current and previous versions are discussed in the current report. The evaluation of the latest Regional Atmosphere version 2 for tropics (RA2T) against the previous version (RA1T) was conducted using IAF/IITM lightning observations as well as 25km resolution satellite-gauge merged rainfall analysis. Later ocean masking was done for the lightning data as the observations were found to have less coverage over the vast oceanic areas surrounding the Indian peninsula. The comparison of gridded statistics for Indian domain covering entire India, but considering land only grid points was operationalised from 1 October, 2021. Comparison of the current masked extended Indian domain (IN) against the previous All India (AI) box also was carried out and presented in the current report.</p>
11	Security classification	Non-Secure
12	Distribution	Unrestricted Distribution
13	Key Words	Lightning forecasts, NCUM-R, ENLS datasets, ocean masking

Contents:

1. Introduction	1
2. Regional model (NCUM-R) upgradation..	2
3. Lightning parameterisation scheme.....	4
4. Merging the lightning flash counts observations.....	5
5. Verification methodology and experimental description.....	6
6. Verification: RA1T vs. RA2T.....	7
6.1 Case study 1: Kerala Floods (2018, 2019).....	7
6.2 Case study 2: 2-12 September 2020.....	11
6.3 Case study 3: Large scale lightning event, 26 June 2020.....	15
7. Impact of All India box computation with ocean masking.....	17
8. Summary and conclusions	18
Appendix-1	
Description of the lightning verification system.....	19
Acknowledgments.....	21
References.....	21

1. Introduction

Over the recent years, lightning has been identified as the single largest killer over India compared to all other natural disasters. There is an increasing trend in death due to lightning. Recent data suggests that lightning alone accounts for about 2,000 to 2,500 deaths every year in India. The Earth Network Lightning Sensor (ENLS) on satellites combined with the ground based observing platforms provide the footprints of deep convective activities at higher spatial and temporal resolutions matching with the convection-permitting models. The high detection efficiency of in-cloud strikes has the potential of improved lead times for severe weather warnings and lightning alerts using total lightning detectors. These observations have opened an avenue for verification and evaluation of very high resolution cloud resolving models. ENLS lightning network systems installed by Indian Institute of Tropical Meteorology (IITM), Pune and Indian Air Force (IAF) were made available in recent times in India for in-cloud lightning detection, which is very valuable dataset for the evaluation of the mesoscale models apart from the evaluation by much coarse resolution raingauge datasets available in India.

Lightning parameterization and lightning potential indices are being developed for very high resolution numerical models to take advantage of the high resolution and independent lightning observations available (Yair et al., 2010; Fierro et al., 2013, Price and Rind, 1994). Traditionally lightning potential is predicted at a station location by computing the various static stability parameters from the radiosonde soundings (Haklander and van Delden 2003; Vujovic et al. 2015; Kunz 2007). However, one of the limitations of this methodology is the unrealistic basic assumption of the homogeneity of the atmospheric layers in space and time. Also beyond any kind of nowcasting potential, its applicability to longer range of prediction is restricted due to the non-consideration of the evolving synoptic conditions like large-scale flow and convergence zones and the synoptic scale lifting triggered by differential vorticity/temperature advection or diabatic heating.

With the advances in the resolution and physics of Numerical Weather Prediction (NWP) models, computation speed and new types of non-conventional observations, it has become possible now, to simulate and develop model products characterising more and more intricate processes in the atmosphere, and to increase the number of prognostic variables including various tracers. Very high resolution mesoscale models are being used to parameterise highly sophisticated explicit cloud electrification processes and generate lightning probability (Dahl et al. 2011; Lynn et al. 2012; Fierro et al. 2013; Choudhury et al. 2020). Alternatively NWP models can generate diagnostics of total lightning as a function of ice mass flux in different convective (precipitating and non-precipitating) and climate regimes (Gungle and Krider 2006; Deierling et al. 2008; McCaul et al. 2009; Yair et al. 2010). A new parameter ‘Lifting Potential Index’ was introduced by Yair et al. (2010) as a threshold value for charge generation and separation between the main charging zone (0°C to -20°C) of the cloud. The key factor to the success of the explicit electrification methods used in convective scale models is all about how accurately we can simulate convective processes and how realistically we can describe the microphysical properties of the clouds.

National Centre for Medium Range Weather Forecasting (NCMRWF) upgraded its Unified modelling system (generally referred to as, NCUM) in 2020, with global model (NCUM-G) in July and regional model (NCUM-R) in October which involved no change in resolution, but a set of science changes in tune with the corresponding versions of United Kingdom (UK) Met Office Unified Model (UM). The upgradation of regional modelling system was carried out after a long period of testing with the regional atmospheric science changes as suggested under the collaborative Regional Model Evaluation and Development (RMED) framework (Jayakumar et al., 2020). The model upgradation involved tuning of the electricity parameterization scheme and validation against the high resolution ENLS datasets. There are two different sources of ENLS datasets available for India, which can complement with each other to some extent over the wide regions of Indian peninsula which traditionally lacks quality data coverage spatially and temporally suitable for very high resolution mesoscale model verification, though it is not clear if the data coverage is uniform throughout the length and breadth of the country for the two sets of data. These observations are recorded with very high spatial and time resolution providing records of lightning flashes in terms of seconds, which are counted for particular space and time slices to indicate a measure of the activity. On the other hand, there can be possibility of some limited data duplications arising out of the simple addition of the number of flash reports from two independent networks over a grid mesh to represent the intensity of the thunderstorm event. An algorithm is developed and is described in this current manual, which is used to generate a merged observation dataset for the demonstration of the model validation. The sections followed describe the model upgradation details, electricity scheme, merging algorithm and the summary of the results from the model validation with respect to lightning flash counts and side-by-side precipitation.

2. Regional model (NCUM-R) upgradation

NCUM-R is adopted from the nesting suite configurations of UK Met Office cloud-resolving models, which are more user-friendly and globally relocatable to any domain over the earth. NCUM-R follows Even Newer Dynamics for General atmospheric modelling of environment (ENDGame) core of dynamic framework (Wood et al., 2014) and has 4km horizontal resolution and 80 vertical levels reaching 38.5km as the top of the model (See Bush et al., 2020; Jayakumar et al., 2021). The domain covers 62°E-106°E, 6°S-41°N and has 1200x1200 grid points extending eastward to include the Bay of Bengal Initiative for Multi-Sectoral Technical and Economic Cooperation (BIMSTEC) countries. Timestep is 2 minutes and the model is run for 75 hours twice a day (00Z and 12Z) and nested with the lateral boundary conditions (LBCs) by NCUM global model (Kumar et al., 2020) at 12km resolution. The model uses rotated longitude/latitude grid for horizontal discretization, with the pole rotated so that the equator runs through the centre of the model domain. Arakawa-C grid staggering is used in the horizontal (Arakawa and Lamb, 1977) and Charney-Phillips staggering is used in the vertical (Charney and Phillips, 1953), while a terrain-following height-based coordinate system is used in the vertical.

There are two flavours of the regional atmosphere (RA) configurations at Met Office each for mid-latitudes (M) and tropics (T). The important differences between the tropical and mid-latitude science settings are mainly on the cloud scheme (diagnostics scheme by Smith (1990) for midlatitude and prognostic cloud and condensate scheme (PC2) for tropics) and the stochastic perturbations for temperature and humidity for midlatitudes (See Bush et al., 2020 for details). Current upgraded version is referred to as (NCUM-R:V4) which is based on the UK Met Office Regional Atmosphere version 2 with tropical science settings (RA2T) version of the nesting suite and which is an upgradation from previous version RA1T. Radiation scheme uses Edwards and Slingo (1996) and land surface processes use Joint UK Land Environment Simulator (JULES) scheme (Best et al., 2011). Gravity wave drag is based on Lott and Miller (1997) and boundary layer processes use a blended scheme (Boutle et al. 2014) which dynamically combines 1-D boundary layer scheme (lock et al., 2000) and vertical turbulence scheme (3D Smagorinsky) with the mixing coefficient of 0.5. The sub-grid scale component of the convection is supposed to resolve the convection and hence deep convection parameterisation is not called. Microphysics is based on Wilson and Ballard (1999) with many modifications and cloud scheme uses Prognostic Cloud and Prognostic Condensate (PC2) scheme (Wilson et al., 2008) along with cloud erosion scheme. Aerosols and chemistry processes are modelled by Coupled Large-scale Aerosol Simulator for Studies in Climate (CLASSIC) scheme (Bellouin et al., 2011) and monthly mean aerosol climatologies are interacting with radiation. Orography is derived from Shuttle Radar Topography Mission (SRTM)~90m) and the land use land cover from International Geosphere-Biosphere Program (IGBP ~1km).

There are a number of science changes between RA1T and RA2T (See Bush et al., 2020). There are changes to the form drag over sea ice and reducing the convective gustiness contribution to surface exchange. The vertical levels of RA2 versions for tropical and mid-latitudes have been unified to 90 levels, whereas in RA1T, it was 80. However, for NCMRWF implementation, the levels have been retained as 80, which is the same as for the previous version (NCUM-R:V3). Changes in the JULES land surface processes include, melting of the snowpack from the base over warm ground and limiting the drag over ocean at high wind speeds. The changes to boundary layer include Leonard flux terms, some bug fixes in Smagorinsky scheme, and use of real fluxes output from JULES scheme for boundary layer type diagnosis (rather than diagnosing the same with surface flux computation before the call to JULES).

Apart from these science changes between RA1T and RA2T as mentioned above, additional local changes are implemented in the NCUM-R:V4 (Jayakumar et al., 2021). Multi-layer snow scheme is introduced in the place of simple (zero-layer) scheme of JULES (Walter et al., 2019). Another modification is on the upgradation of the visibility parameterisation scheme in NCUM-R, where originally the aerosol mass mixing ratio (m) is assumed to be fixed for RA1T version. In the current version the visibility scheme was modified to use aerosol climatologies which affect the computation of m . A tuning factor of 2 has been applied to the aerosol number concentration, which has a feedback on the visibility diagnostics but do not affect the science or the model simulations. The surface layer cloud

droplet number tapering is switched off in the current implementation as the aerosol content in India is generally too high. Also there is a change in the threshold for storm detection at a grid point to invoke the lightning parameterisation at a grid point as a part of tuning of the scheme, which is discussed in the next section.

3. Lightning parameterisation scheme

Cloud microphysics scheme in the model describes the ice and graupel processes (Wilson and Ballard, 1999; Wilkinson et al. 2020; Zerroukat and Shipway, 2017) and hence the lightning potential can be diagnosed by explicitly modelling the cloud electrification processes or by statistical relationships between the observed lightning flash rate and the total ice content in the atmospheric column (McCaul, et al., 2009). Another statistical relationship is also being used to correlate with the updraft graupel flux in the mixed-phase level ($\sim -15^\circ\text{C}$ level). The sound scientific reasoning behind these statistical correlations is based on the underlying processes behind the lightning generation, that there should be a co-existence of super-cooled water droplets, ice/snow crystals and large-sized graupel crystals to generate lightning flashes. The strong updraft above the freezing level of the convective storms causes rising ice crystals to grow into large-sized snow crystals, which become large enough to fall through the atmospheric column. The differential fall-speed of the particles cause more collisions to happen and the falling snow crystals grow into graupel due to accretion in the presence of super-cooled water droplets. The part of cloud with rising ice crystals and those with falling graupel attain opposite polarity which leads to the start of cloud-to-cloud (CC) discharges which eventually grow up to the large scale so that the positively charged clouds and the negatively charged earth surface features will get discharged to cause cloud-to-ground (CG) lightning.

Sandeep et al. (2021) describe the electric scheme in NCUM-R which is based on McCaul et al., (2009) , which is a blended version to capitalize on the strength of two empirical relationships between the flash rates and two independent cloud microphysical properties. Thus the flash rates are proportional to graupel flux at mixed-phase level of -15°C and the total volumetric amount of precipitating ice, which are combined together to obtain the following formulation.

$$F = 0.95 * k_1 (wq_g)_m + 0.05 * k_2 \int \rho (q_g + q_s + q_i) dz \quad (1)$$

$k_1 = 0.042 \text{ m}^{-1}$ is lightning-graupel flux factor; $k_2 = 0.20 \text{ kg}^{-1} \text{ m}^2 \text{ s}^{-1}$ is lightning-storm ice factor. w denotes vertical velocity, ρ air density and q_g , q_s and q_i represent the mixing ratios of graupel, snow and ice respectively. The subscript ‘m’ denotes the mixed layer height of -15°C and dz is the vertical displacement.

The lightning scheme is invoked at the grid points wherever the graupel water path exceeds a threshold value of 200 gm^{-2} in RA1T. Also there was an option to use snow-rain collision to generate graupel with the implications of more flash potential (Sandeep et al.,

2021). In RA2T it was found that the flash counts were predicted less compared to RA1T and sometimes it is missing over the regions of moderate lightning regions. So a number of experiments were conducted to increase the flash counts of RA2T to be mostly at par with RA1T at least in terms of area coverage. The most effective way was found to reduce the GWP threshold to 100gm^{-2} for storm detection which was used as experimental configuration for RA2T. A number of case studies of various intensities were used for testing the sensitivity of the science changes and finally adopted the reduced threshold for the operational implementation.

With the availability of highly dense lightning observation networks by IAF and IITM, the peak intensity, location and timing of the total lightning flash rates (CC+CG: Cloud-to-cloud + cloud-to ground) can be verified. The ENLS observations can detect both CC and CG flash counts. The low frequency (1 kHz) is used for longrange detection of CG discharges. The middle frequencies (1 kHz to 1 MHz) are used for locating return strokes, and the highest frequencies (1 MHz to 12 MHz) are used to detect and locate in-cloud pulses. If the strokes are within 700 milliseconds around 10 km, then it is clustered into a flash and a flash that contains at least one return stroke is classified as a CG flash. The detection efficiency of the ENLS CG flashes is 90% and for CC flashes it is 50% (Mohan et al., 2021). The observations and model diagnostics can be converted into 3hrly accumulated flash rates at $4\text{km} \times 4\text{km}$ resolution. Both the 24 hour accumulated flash counts and 3 hourly snapshots are verified using standard verification measures, though only 24-hourly statistics were used in the current study. The description of the operational implementation of lightning verification system is given in appendix – 1.

4. Merging the lightning flash counts observations

. Sandeep et al. (2021) adopted a methodology to merge the two sets of ENLS datasets (IAF and IITM) by simply binning the reports over the $4\text{km} \times 4\text{km}$ grid mesh and finding out the total counts for both the datasets to represent the intensity of the activity at that grid point. This can raise some question mark on possible double counts. Though the double counts can not be avoided completely, it is necessary to develop some algorithm to put some checks on the total flash counts at a grid point. The lightning flashes in nature can occur every second and the range of flashes seen by the ground based stations need not be distinct over a geographical distance of a few kilometers but may be a combined flash (a combination of many high frequency plasma discharges or strikes) can be observed as a long single flash. Also the length of the individual channels lightning discharges can be varied and so there is no thumb rule that can be set about the number of flashes reported in a minute. However, as a compromise, a spatial-temporal criteria can be set as one kilometer and every one minute as bounds, based on which an algorithm was developed to arrive at a reasonable counts for every grid point as a representative of the lightning activity. This algorithm is an important modification as far as the evaluation and verification is concerned compared to the previous study (Sandeep et al., 2021).

The algorithm developed to merge the flash counts from both the sources of datasets is as follows. Once IAF data is read in, then they are matched pairwise with each IITM

observations. If both of them are within 1km distance with each other in the same minute, only one is counted and the extra one flash count is neglected to avoid possible double counting of the same event. Also the flash counts reported in delayed mode for the current day in the next half hour soon after the end of the day are also counted for the current day. This algorithm is found to reduce the 24 hourly accumulated flash counts over All India domain, by maximum 10% on average and the peak counts at any particular grid by maximum around 2%. So apparently the impact of this procedure is very minimal, but still very important as a common protocol to be adopted for the merging of any future datasets over the same domain. The process is more time consuming and was provided considerable speed up with a few efficient measures of parallelism and compute node level work allocations. The current study uses this merged dataset for the verification statistics.

5. Verification methodology and experimental description

A number of cases were simulated and compared between RA1T and RA2T (with two runs: Ctl and Exp1). Comparison study of Kerala floods during August 2018 and August 2019 was conducted with the study periods, 5 days ICs each of 12-16 August 2018 and 8-12 August 2019 respectively, selected. All types of objective scores were computed along with Fractions Skill Score (FSS) and developed High Resolution Assessment (HiRA) scorecards with different thresholds versus different neighbourhood sizes for 24-hourly accumulated precipitation and lightning flash counts. Fig. 1 shows the peak rainfall days for both the episodes valid for 03Z of 15 August 2018 and 9 August 2019 with the boxes shown are the domain for averaging (68-88°E, 8-28°N), which excludes the Himalayas, north-east India and data sparse remote oceanic regions to get relatively matching coverage for corresponding observations against the model grid points. The thresholds used for precipitation are 1, 10, 20, 40, 80, 160, 320 mm and for lightning counts are 1, 5, 10, 20, 30 and 50. The observations used are 25km resolution merged rainfall analysis (which is the most reliable data available) and high resolution IAF/IITM Earth Network Lightning Sensor (ENLS) lightning flash counts (only for August 2019 only as there are no lightning observations available for August 2018).

Two sets of experimental runs of varying domain profiles were carried out for the lightning verification system as follows:

- i) Exp1: All India domain (AI) but avoiding Jammu and Kashmir, north-east India and much of the vast oceanic areas (68-88°E, 8-28°N).
- ii) Exp2: All India domain (IN) which touches all the four Indian boundaries, but masking the oceanic areas (68-97°E, 8-37°N).

There are three case studies presented in the current document with different synoptic conditions. They are with ICs for (1) Kerala floods case of 12-16 August 2018 and 8-12 August 2019, (2) 1-11 September 2020, and (3) large scale Uttar Pradesh-Bihar lightning event during which large casualties were reported (25 June 2020). The runs were made with

downscaled initial and boundary conditions from the NCUM global model analysis and forecasts. The results of the experiments Exp1 are discussed in the section 6 and Exp2 are discussed in section 7.

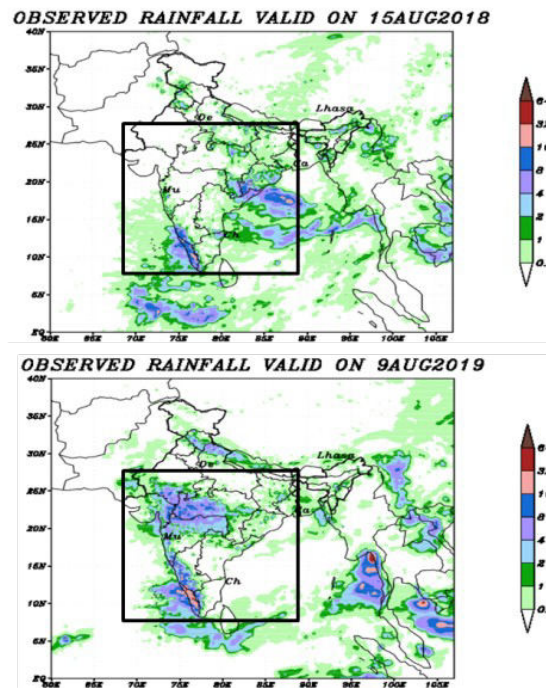


Figure 1 Observed rainfall (cm/day) for the peak rainfall days of (a) Kerala floods 2018 (15 August) and (b) 2019 (9 August) with the domain boxes (68-88E, 8-28E) for averaging the statistics.

6. Verification: RA1T vs. RA2T

6.1 Case study 1: Kerala Floods (2018, 2019)

Two active monsoon periods causing major flood event in the southern-most state of Kerala were compared to study the impact of the science changes between RA1T and RA2T. Five days were selected each of the years 2018 and 2019 during the active Monsoon period and centered on the flood events (13-17 August 2018 and 9-13 August 2019). Spatial distribution of average rainfall for these periods is shown in Fig. 2, which shows the rainfall from the forecast extrapolated to a common observation grid resolution (25km) using the series analysis tool of Model Evaluation Tool (MET) software (Fowler et al., 2017). This tool accumulates statistics separately for each horizontal grid location over a series. Often, this series is over time or height, though any type of series is possible. This verifies all grid locations together as a group rather than taking a domain average. Rainfall distribution is comparable between the two experiments (a & b) though western ghats (WG) rainfall is somewhat overprediction over north Kerala and south coastal Karnataka in RA2T compared to RA1T. RA2T features higher peaks over these regions. Whereas the rainfall over Gujarat and Maharashtra is a better match with the observations for RA2T compared to much drier RA1T. The rainfall coverage is over predicted over Chhattisgarh and Odisha in both RA1T

and RA2T compared to the observations. These are reflected in Root Mean Squared Errors (RMSEs) (d and e) with higher RMSEs for RA2T compared to RA1T owing to the double penalty problem. Bias (Mean Error:ME) for RA2T (f) also shows similar pattern as RMSE (e) but indicates overall a slight positive bias for RA2T over most parts of the domain as denoted by greenish shades.

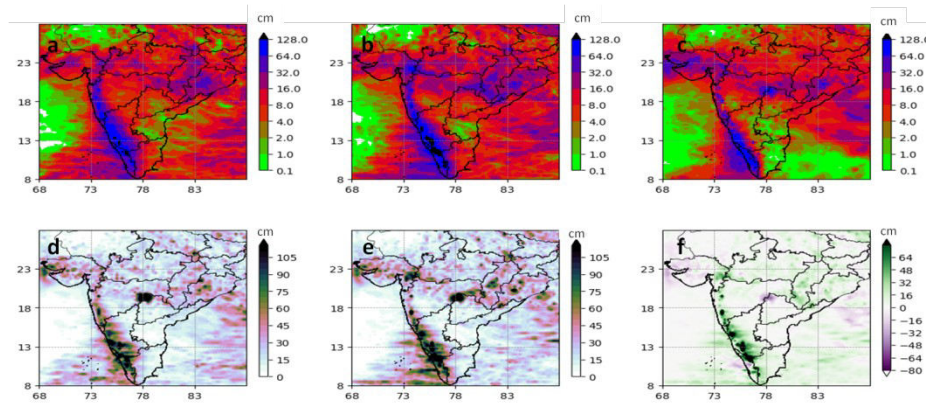


Figure 2 Total precipitation (cm/day) averaged for the Kerala floods (9-13 August 2018 & 13-17 August 2019) for (a) RA1T (b) RA2T and (c) IMD-NCMRWF satellite-gauge merged rainfall along with average spatial distribution of the root mean square error for (d) RA1T (e) RA2T and (f) mean bias for RA2T.

Fig. 3 compares both rainfall (a – c) and lightning distribution (d - e) for 2018 episode, whereas no observations were available for lightning flash counts verification. Most of the features are similar to the combined episode, whereas over Maharashtra, the coverage and intensity of rainfall are better reproduced by RA2T compared to RA1T, even though the

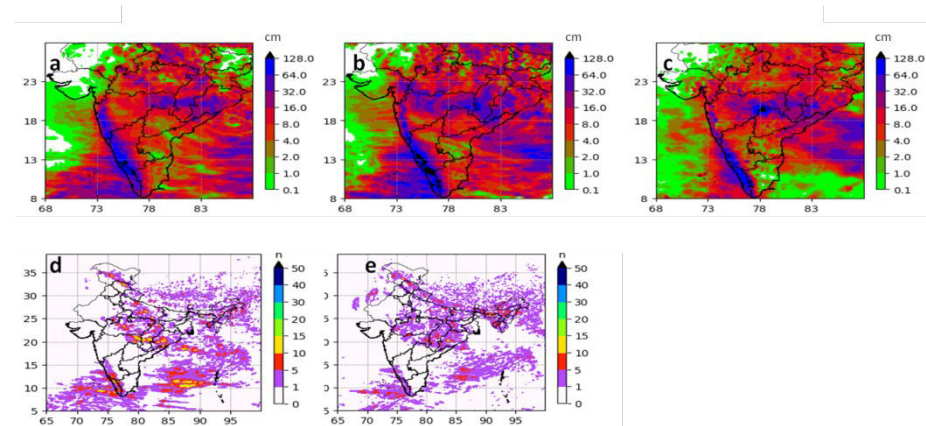


Figure 3 Total precipitation (cm/day) averaged for the Kerala floods (9-13 August 2018) for (a) RA1T (b) RA2T and (c) IMD-NCMRWF satellite-gauge merged rainfall along with average total lightning flash counts spatial distribution for (d) RA1T and (e) RA2T.

hot spots observed over Maharashtra-Telangana border is missing in either simulations. As far as lightning distribution is concerned, RA2T coverage is more over land areas, whereas RA1T features slight over prediction at some of the hot spots for lightning flash counts (~30 per day) over Maharashtra, Chhattisgarh, Odisha and Kerala. Fig. 4 is also similar to Fig. 3, but for 2019 case study. Here also we can see heavy rain hot spots over the WG, especially over south central Karnataka and Kerala border for RA2T. Importantly the hot spot seen in the middle of Kerala is not represented by any of the experiments in terms of location, except

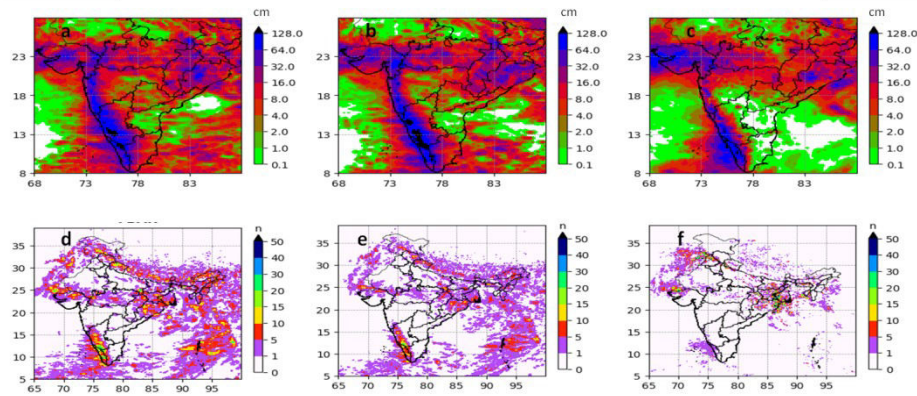


Figure 4 Total precipitation (cm/day) averaged for the Kerala floods (13-17 August 2019) for (a) RA1T (b) RA2T and (c) IMD-NCMRWF satellite-gauge merged rainfall along with average total lightning flash counts spatial distribution for (d) RA1T, (e) RA2T and (f) IAF/IITM ENSL datasets.

some hot spots over the top of orography in RA2T compared to totally missing case of RA1T. Overall it can be concluded that central India rainfall is better predicted in RA2T compared to RA1T whereas the remaining distributions are more or less comparable between the two versions. As far as lightning distribution is concerned, the models are showing more coverage and intensity compared to the observations over the western Ghats coastal belt, and the peak hotspots are much widespread for RA1T compared to RA2T. It can also be seen the large spread of lightning flash counts predicted for the vast stretches of oceanic region and over the Himalayas, especially with high intensity hot spots in RA1T. To summarise, it can be concluded that since the detection efficiency of the ENLS network may be 70-80% only (and hence can be little underestimated in the observations), the predicted flash counts over the major areas of eastern, western and northwest are fairly matching with the observations.

Fig. 5 shows comparison of domain averaged statistics (difference in Fractions Skill Score) for rainfall (2019 (a), 2018 (c) and both combined (b)) as well as flash rates (2019 (d)). The rectangular box denotes 5 grid width statistics for all the thresholds. It can be seen that RA2T shows improved rainfall statistics for 2018, neutral for 2019 and overall improvement for both combined. Flash counts for 2019 show improved scores for RA2T at lower thresholds, while at the extreme thresholds show some degradation. This may be due to the lower counts of peak grid points of flash counts in RA2T compared to RA1T, but still what is important is that Yes/No forecast is better in RA2T with larger area coverage of lower thresholds. Similarly, Fig. 6 shows the Critical Success Index (CSI), Equitable Threat Score (ETS or GSS), and False Alarm Ratio (FAR) scores averaged for both years combined for rainfall, which shows slightly less skill for RA2T compared to RA1T at thresholds of 0.1

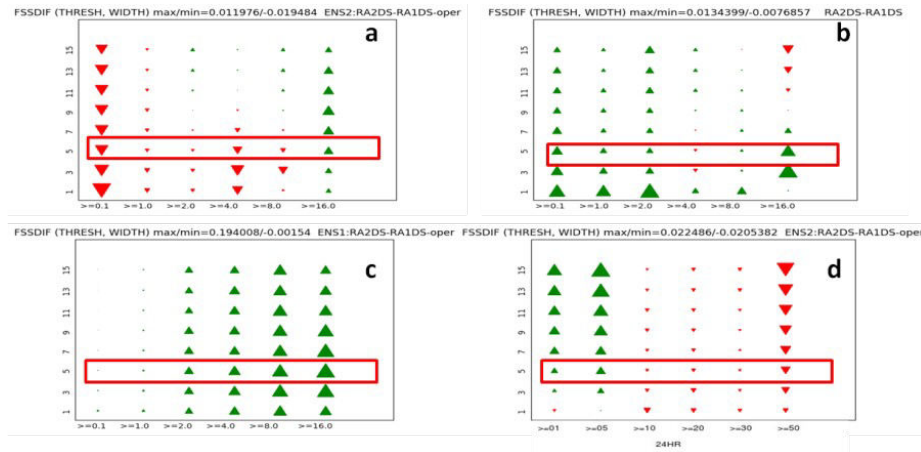


Figure 5 Difference in precipitation (cm/day) Fractions Skill Score (RA2T-RA1T) for ensembles of (a) 2019, (b) 2018 & 2019 (c) 2018 and (d) difference in lightning flash counts Fractions Skill Score for 2019, averaged over the domain 68-88°E, 8-28°E.

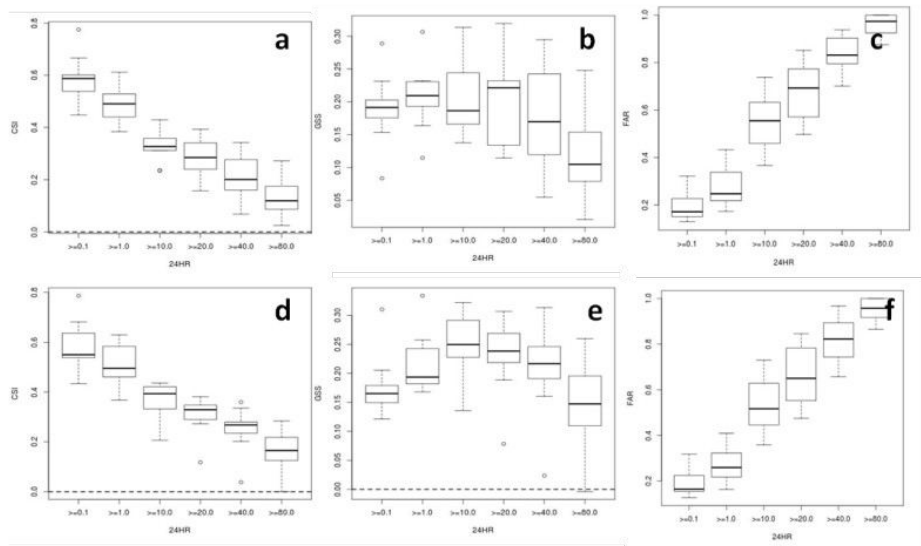


Figure 6 The skill scores (Critical Success Index (CSI), Equitable Threat Score (ETS) and False Alarm Ratio (FAR)) for RA1T (a, b and c) and for RA2T (d, e and f) respectively for total precipitation (cm/day).

and 1cm, but more skill for most of the higher threshold levels. Table 1 shows the domain averaged standard objective verification scores of RA1T and RA2T for RMSE, Correlation Coefficient (CC), Bias (ME), Multiplicative bias (MBIAS) as well as domain mean forecast and observations. It can be concluded that all the scores are favouring RA2T compared to RA1T with all the errors reduced and the correlation increased. The mean forecast values show comparable values between RA1T and RA2T for both rainfall and flash counts, but both are overprediction compared to domain mean observation. However, RA2T is closer to the observation compared to RA1T.

Table 1 The scores for lightning and precipitation for the case 2-12 September 2020 for RA1T and RA2T.

Statistics	LIGHTNING		PRECIPITATION	
	RA1T	RA2T	RA1T	RA2T
RMSE	8.745589	8.336644	28.395639	27.082565
Corr. Coef.	0.032567	0.039343	0.214445	0.237801
Bias	0.452464	0.299027	0.35533	0.250196
Mult.Bias	1.673237	1.495751	1.120515	1.10974
Mean Fcst	1.46396	1.310521	9.888377	9.783241
Mean Obs	1.011495	1.011495	9.533045	9.533045

6.2 Case study 2: 2-12 September 2020

Total Precipitation shows comparable spatial distribution between RA1T and RA2T (Fig. 7). Both show some pockets of rainfall over interior Maharashtra which is not in the observations. Some reduction in RMSE is seen over Odisha in RA2T compared to RA1T. Difference in Fractions Skill Scores (FSSDIF) for 24, 48 and 72hour accumulated precipitation (RA2T-RA1T) for the averaging domain of (68-98°E, 8-28°N) and averaging period of 2-12 September 2020 are plotted in Fig. 8, with x-axis denoting various thresholds and y-axis different neighbourhood sizes. FSS for RA2T shows improvement for all lead times compared to RA1T for total precipitation. Maximum improvement in FSS is seen for 48 hour while minimum improvement in 72 hour for this particular ensemble simulations.

Lightning scheme will be invoked based on the threshold value of GWP (200gm^{-2}) (in the control (Ctl) simulation). Fig. 9 shows the spatial distribution of lightning flash counts, RMSE and bias (ME) against the ENLS datasets. Lightning flash counts are found to be notably reduced all over in RA2T compared to RA1T especially over east India and over western ghats (WG) which are reflected in the RMSEs also. FSS for RA2T shows overall improvement for Day-1 and Day-2, and reduced skill for Day-3 compared to RA1T (Fig. 10). Maximum improved performance is seen in the lower intensity thresholds for Day-1 and some positive impact is also felt at medium to high intensity thresholds for Day-2. Fig. 11 shows the impact of the experiment (Exp1) with reduction in the threshold GWP for invoking the lightning scheme on RA2T. Fig 11(a) is the control FSSDIF (RA2T(Ctl)-RA1T) with GWP threshold of 200gm^{-2} and Fig 11(b) represents the experiment (RA2T(Exp1)-RA1T) with GWP threshold of 100gm^{-2} in RA2T. There is a general improvement in FSS at all thresholds and all grid widths and the maximum improvement of yes/no forecast at 15 grid width is 0.037 for Ctl and 0.49 for Exp1 compared to RA1T in Day-1. Also Fig.11(c-e) shows the improvement in FSS for RA2T between the experiments (Exp1-Ctl) for days 1-3, where we can see an overall improvement at higher grid widths and medium thresholds. At lower

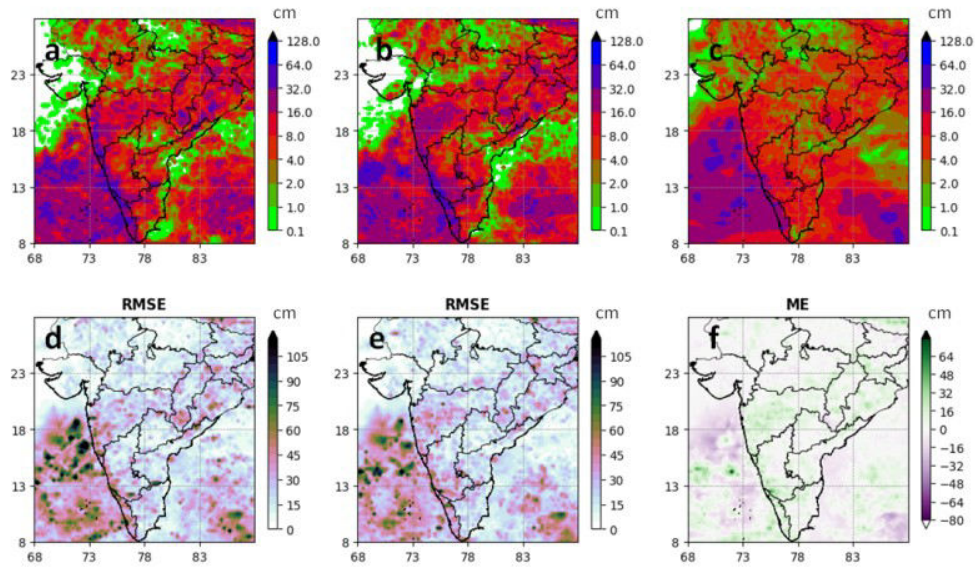


Figure 7 Spatial distribution of total precipitation (cm/day) for the period 2-12 September 2020 for RA1T (a), RA2T (b) and IMD-NCMRWF merged rainfall analysis (c). The lower panels show the spatial distribution of root mean square errors (RMSE) for RA1T (a) and RA2T(b), along with the mean bias (ME) for RA2T.

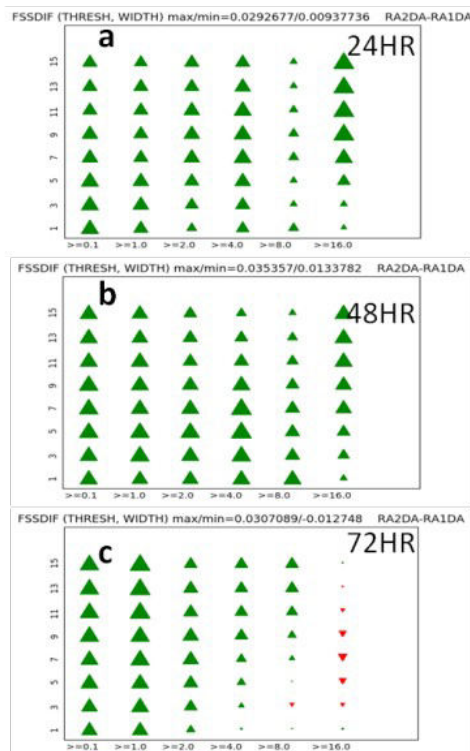


Figure 8 Difference in Fractions Skill score (FSS) between (RA2T-RA1T) for total precipitation (cm/day) for (a) 24 hour, (b) 48 hour and (c) 72 hour lead times averaged over AI domain (68-78E, 8-28N).

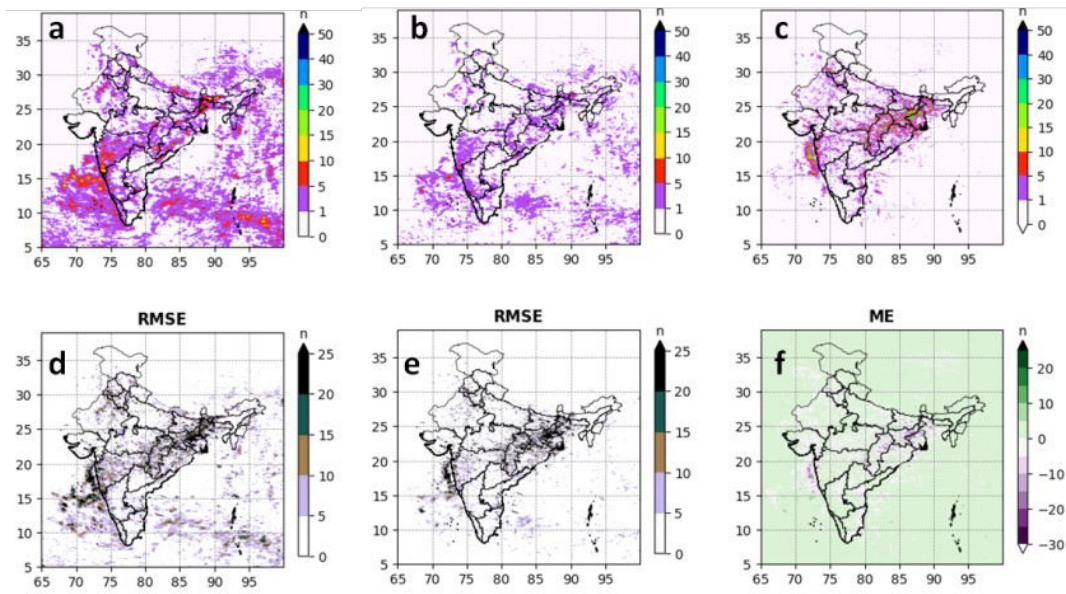


Figure 9 Spatial distribution of total lightning flash counts (/day) for (a) RA1T, (b) RA2T and (c) IAF/IITM ENLS datasets averaged for 2-12 September 2020. The lower panels are root mean square errors (RMSE) for (d) RA1T and (e) RA2T along with (f) the mean bias (ME).

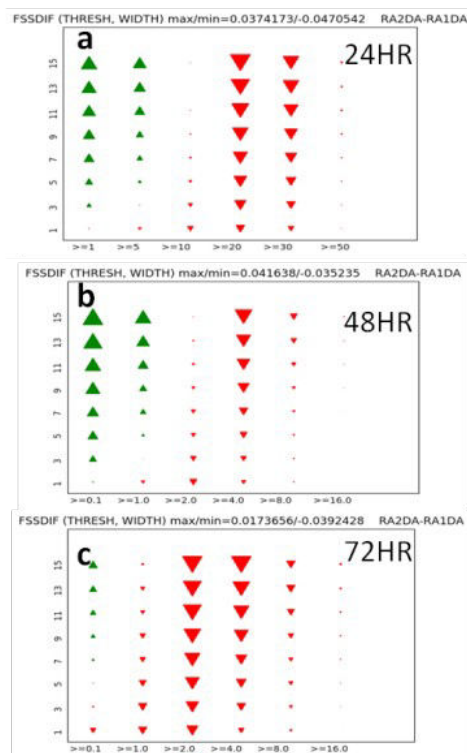


Figure 10 Difference in Fractions Skill score for total precipitation (cm/day) between (RA2T-RA1T) for the period 2-12 September 2020 for (a) 24 hour, (b) 48 hour and (c) 72 hour lead times.

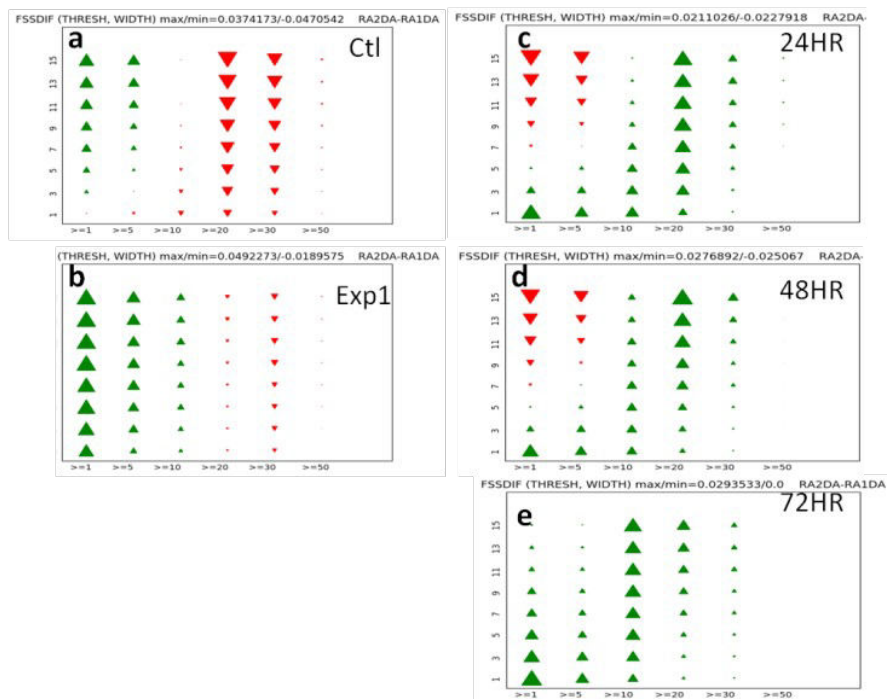


Figure 11 Difference in FSS for lightning flash counts (RA2T-RA1T in units /day) averaged for 2-12 September 2020 for the experiments (a) Ctl and (b) Exp1. The Panels on the right displays the FSS difference (Exp1-Ctl) for lead times (c) 24 hour, (d) 48 hour and (e) 72 hour.

thresholds there is improvement for small grid widths while reduction in skill at higher grid widths. However, at 72 hour forecast lead time the reduction in skill at higher gridwidth and lower threshold is absent and there is an overall improved skill at all thresholds/windows for Exp1 compared to Ctl. Figs. 12 & 13 are similar to Figs. 9 & 10 except for the experiment Ctl replaced by Exp1. Lightning flash counts spatial distribution (Fig. 12a & 12b) looks similar between RA1T and RA2T with reduced GWP threshold (Exp1), which is a good improvement when compared with the

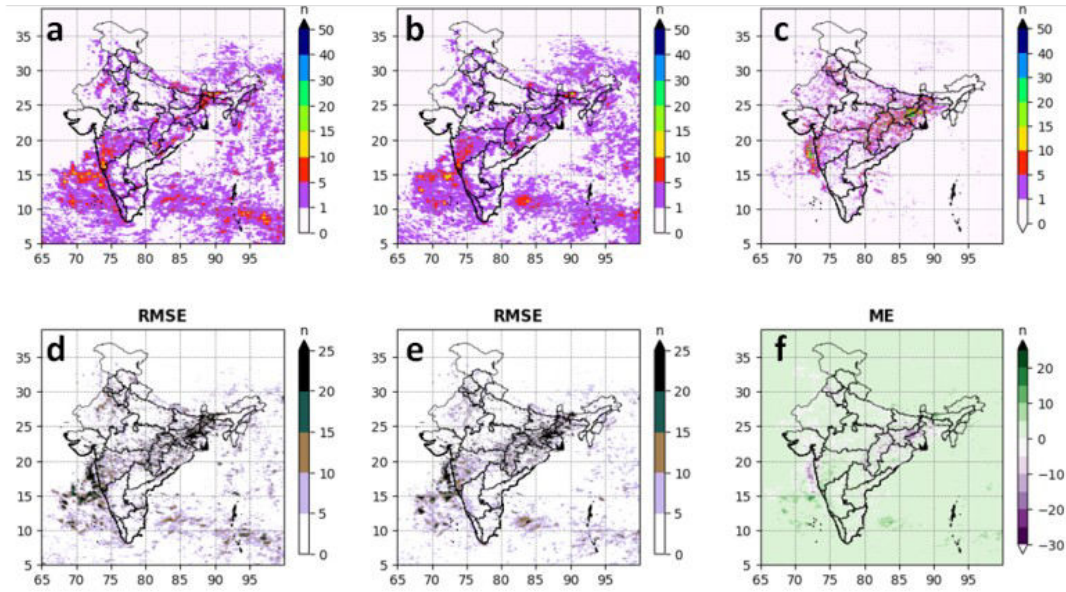


Figure 12 Spatial distribution of total lightning flash counts (/day) for (a) RA1T, (b) RA2T (Exp1) and (c) IAF/IITM ENLS datasets averaged for 2-12 September 2020. The lower panels are root mean square errors (RMSE) for (d) RA1T and (e) RA2T along with (f) the mean bias (ME).

control run of RA2T. Also reduced error can be seen over land for RA2T especially over the west coast of Indian peninsula (Fig. 12e). RMSE also shows in general slight reduction in spatial distribution for RA2T. FSS shows overall improvement for Day-2, while for Day-3 yes/no prediction at lower threshold has improved, while there is a reduction in skill for the medium thresholds (Fig.13). Skill scores are shown in Fig. 14, where it can be observed that CSI and ETS are generally higher for RA2T and FAR is lower compared to RA1T. In general, the skill scores are higher for RA2T (Exp1) compared to RA1T and RA2T (Ctl).

6.3 Case study 3: Large scale lightning event, 26 June 2020

Another case study of large-scale organized, highly intense lightning events which occurred at several places over Bihar and West UP (26 June 2020) shows fairly good performance in capturing the area coverage of the intense activity for day-1 simulations for RA1T and RA2T(Exp1) (Figs. 15 and 16 respectively). The panels (a and b) show same as that in (c and d) with the box region projected. It can be seen that the intense observations and the area coverage are well represented in both runs, but RA2T (Exp1) features better match with the hot spots predicted much better over north-west Bihar, though with a slight eastward displacement compared to the observed distribution. Intense flash counts over Gangetic West Bengal and other north-eastern states as well as those over Jharkhand are better matching with RA2T though the peak values are relatively under predicted. This shows the capability of the model to produce reasonable distribution of the lightning flash counts to save the lives

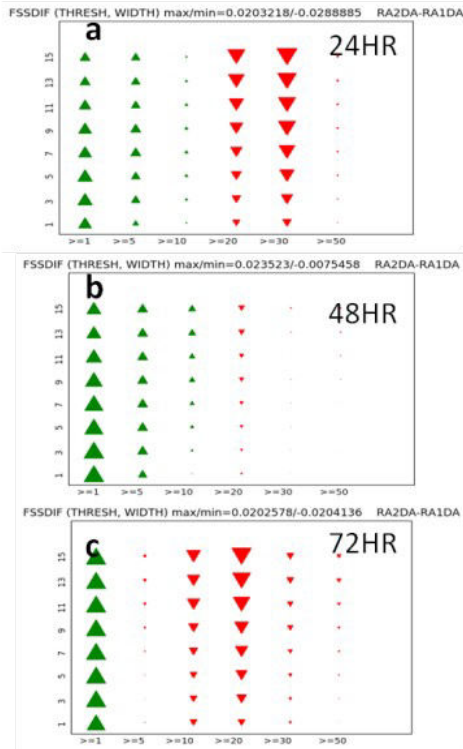


Figure 13 Difference in Fractions Skill score for total precipitation (cm/day) between (RA2T(Exp1)-RA1T) for the period 2-12 September 2020 for (a) 24 hour, (b) 48 hour and (c) 72 hour lead times.

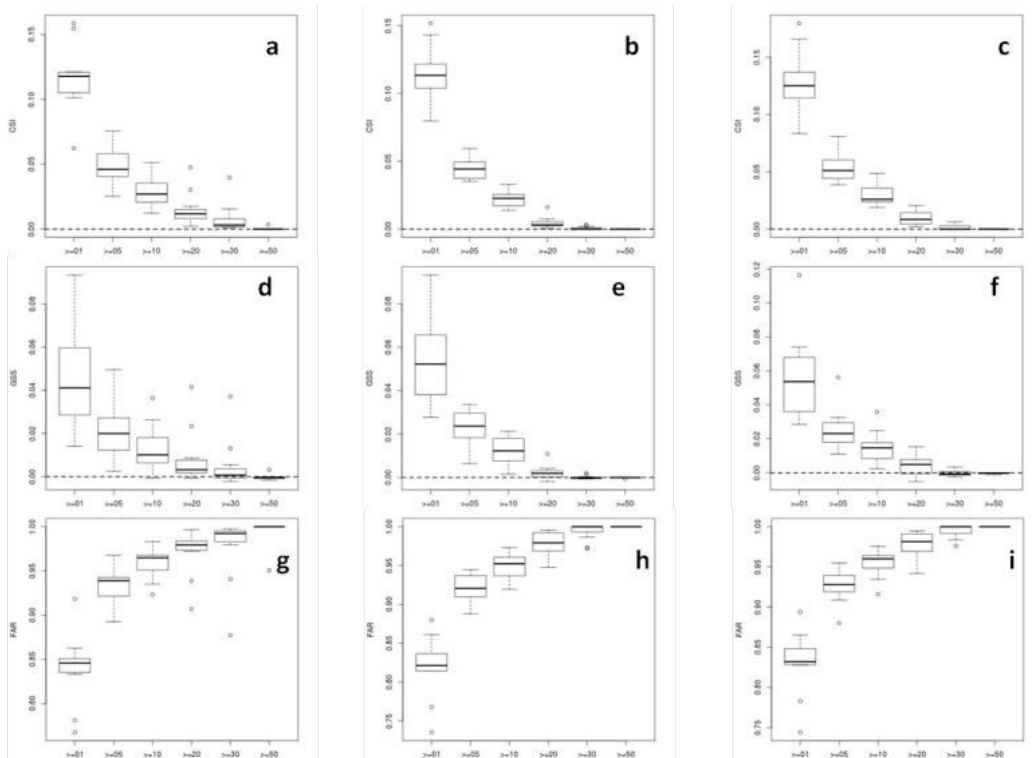


Figure 14 Critical Success Index (CSI – Panels a-c), Equitable Threat Scores (ETS – panels d-f) and False Alarm Ratio (FAR – panels g-i) for RA1T, RA2T(Ctl) and RA2T(Exp1) experiments for total lightning flash counts (/day) averaged for (68-88°E, 8-28°N).

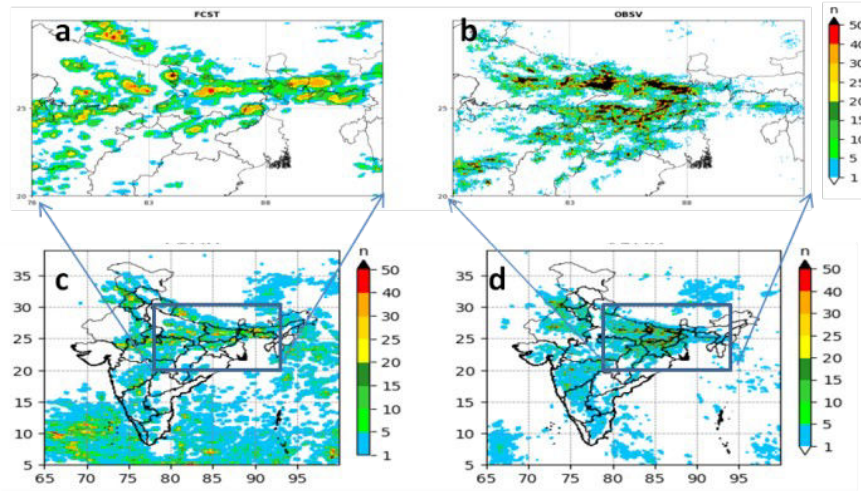


Figure 15 Lightning event on 25 June 2020 over Uttar Pradesh and Bihar: Spatial distribution of total lightning flash counts (/day) for (c) RA1T and (d) IAF/IITM ENLS dataset, which is projected over the eastern Indian domain box in (a) and (b).

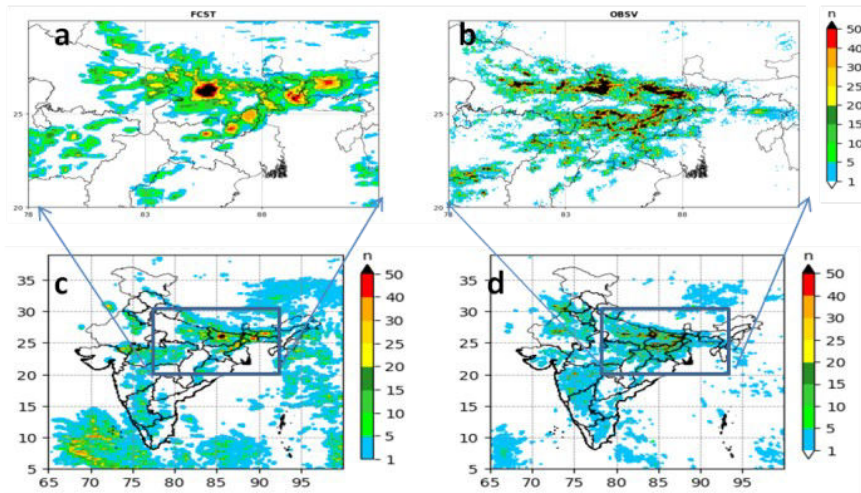


Figure 16 Similar to Fig. 15 except for RA2T (Exp1).

along with an efficient communication mechanism to alert the affected population. With RA2T (Exp1) there is a significant improvement in the flash intensity as well as location compared to RA1T.

7. Impact of All India box computation with ocean masking

It is observed that the observation coverage over the oceanic regions are limited and distributed more close to the land regions compared to the model forecast areal spread. The high bias over oceanic regions for the model forecasts may likely to lead to slightly biased conclusions when taking the domain averages for gridded statistics, even though the impact is

reduced by taking a more restricted box rather than a literally All India domain. Also by avoiding the Jammu and Kashmir and west Himalayan region as well as north-east India, the statistics ignores the western disturbance events over the western Himalayas and the highly frequent thundershowers of north-east India. Hence it was decided to extend the averaging domain box to include these important sectors and mask the oceanic areas to limit the statistics for land only, which will be of more useful and realistic for the model evaluations and policy making. This was implemented from 1 October, 2021 operationally and this includes generating a mask file ‘oceanmask.nc’ using a python script which sets grids over land as ‘1’s and over ocean as ‘0’s with a single change in the grid_stat configuration file with the mask definition as follows:

```
mask = {
    grid = [ ];
    poly = [ “/full-path-to-maskfile/oceanmask.nc” ];
};
```

Fig. 17 shows the FSS scores over Indian domain (IN) for Exp2, during 2-12 September 2020 for RA2T without (NOMASK) and with ocean-masked (MASK) values for first 24 hourly accumulated lightning flash counts, which shows the improved scores with ocean-masking for both maximum and minimum ranges compared to that with no masking. Hence in general it is demonstrated that the ocean masking is able to produce more realistic skill of the lightning flash count prediction over the land region which will be very useful for both the policy makers and scientists.

8. Summary and conclusions

Regional NCUM model was successfully upgraded from RA1T to RA2T in October 2020. Simultaneously a lightning verification system was operationalised at NCMRWF after the development of a more efficient technique to merge the IAF and IITM lightning sensor observations. This indigenously developed merging technique is based on the simple logic of avoiding the possibility of duplications in the two similar ENLS networks of IAF and IITM if it occurs within a minute and a kilometer distance apart. This procedure is found to avoid a possible duplication of the lightning flash counts which are of very high spatial and temporal frequency. This logic has a potential to be extended to merge any number of datasets in future to make a mosaic of the flash counts. Overall standard scores for accumulated rainfall shows improved performance for RA2T compared to RA1T at all thresholds and all scales. However the lightning flash counts were overpredicted by NCUM-R compared to observations for RA1T while slightly underpredicted by RA2T. A tuning was applied to lightning scheme by lowering the threshold of graupel water path from 200 gm⁻² to 100gm⁻² for invoking the lightning scheme at a grid point. Experiments with the modified lightning scheme show comparable skill of RA2T similar to RA1T after the tuning, and with less overprediction. The ‘land only statistics’ over All India domain including Jammu and Kashmir and north-east

India, but with the oceanic region masked produces improved scores for lightning flash counts with less bias due to more spread of model forecasts over oceanic region.

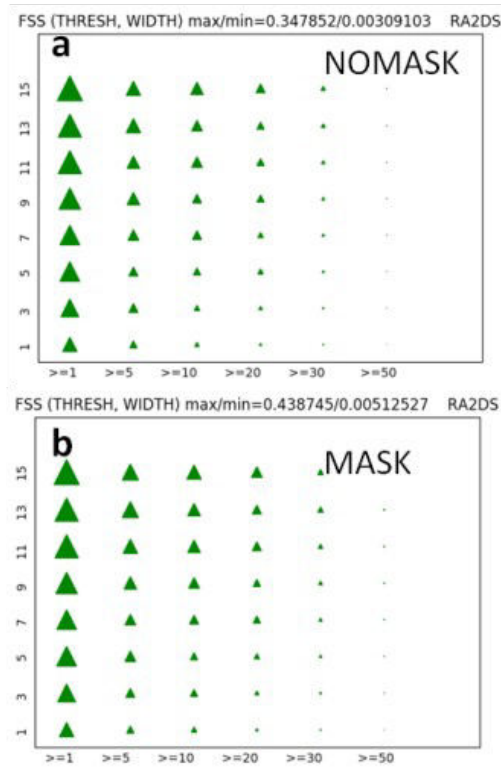


Figure 17 Fractions Skill Scores of lightning flash counts (/day) for RA2T (Exp2) for the All India domain (68-97E) and (8-37N) (a) with inclusion of the oceanic regions unmasked and (b) with oceanic regions masked (land only averaging) averaged for the simulation period 2-12 September 2020.

Appendix – 1

Description of the lightning verification system

The root directory for the NCUM-R lightning verification system is named as LIGHTNING_verify. The flow chart of the LIGHTNING_verify is given in Fig. 18. The tool has three sections, namely prod, stats and plot. The folder prod extracts the lightning data in collocated 4kmx4km grid structure for the domain. This is done by a python program 'IAFobsvsNCUMRfest_4by4km_daily_3hrly.py'. Both the collocated model forecast and observations are written in netcdf format which are used by stats section for the computation of the gridded statistics using 'grid_stat' tool and time-averaged spatial distribution by series analysis tool. MET7 is used for the computation of the statistics and is the latest MET version using Python 2.7 for Python embedding to prepare 2D gridded data fields for reading by MET tool. The gridded statistics generates both standard objective scores including the neighbourhood scores (For a description of the objective skill scores and the output file types

produced by ‘grid_stat’ tool in MET7, please refer to the documentation by Fowler et al., (2017)). The output is stored in output folder separately in sub-folders for 24HR, 48HR and 72HR. Also the netcdf files of the observations are stored in OBSV folder.

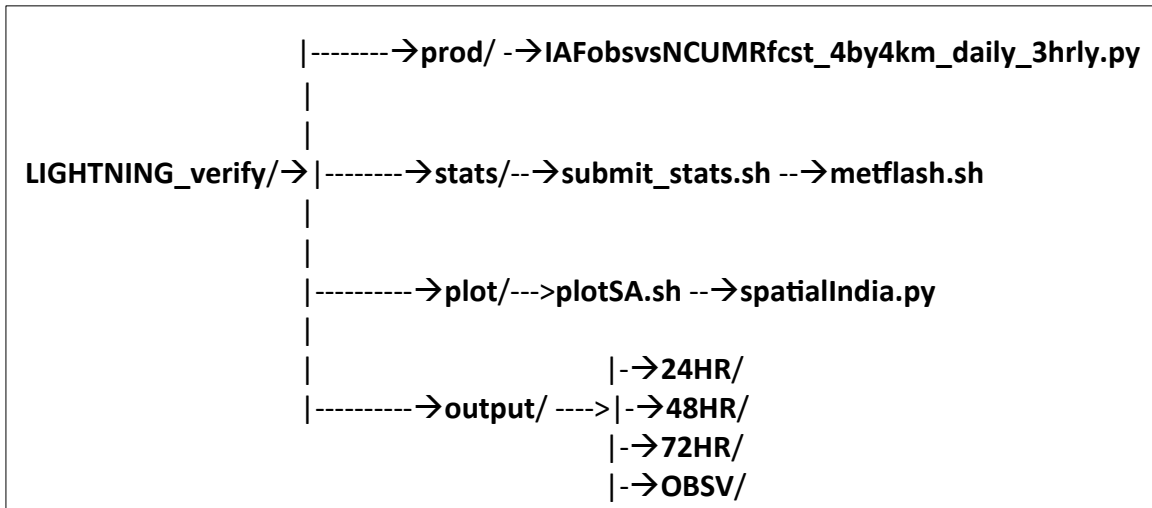


Figure 18 Flow diagram of the lightning verification system with the subdirectories prod, stats and plot for the computation and graphical visualization and output folder for saving the data, tables and figures for observations, and forecasts of lead times 24, 48 and 72 hours.

The entire computation can be submitted by a single command by entering the ‘prod/’ folder and issuing command;

```
./submit.sh YYYYMMDD ZZ LEAD
```

Where YYYYMMDD is the date stamp, LEAD the lead time (24/48/72) and ZZ is the cycle (00/12). ‘submit.sh’ script in ‘prod’ folder calls another three scripts ‘prod_run’, ‘stats_run’ and ‘plot_run’ which are optimized and parallelized to be executed fast to generate the input datasets in netcdf format, computation of statistics using MET7 and spatial plotting of the observations against forecast. The generation of the observed and forecast gridded lightning data at 4kmx4km resolution is done by the python program. Then the statistics computation using MET7 is done in ‘stats’ folder. This computes the statistics and store in output/FH’hr’ folder where FH is the Forecast Hour ranges under different folders like 24-hourly accumulation in ‘00-24hr’, and at 3-hourly intervals in folders ‘00-03hr’, ‘03-06hr’... and so on. Also it dumps netcdf files for forecast (fcst.nc), observation (obsv.nc) and combined (SAout.nc). The script metflash.sh employs two tools (grid_stat and series_analysis) for the generation of standard objective scores and spatial averaged distribution of some of the statistics (RMSE and ME). The final stage is ‘plot’ folder which prepares graphic visualization of the spatial distribution of predicted lightning and the measures and stores the image in the same folder in the name ‘LIGHTNING_spatial_stats.png’. The following set of ascii tables are generated for various

kind of objective scores (like contingency table statistics and continuous statistics) as follows (for IC: 00Z, 2-10-2021);

grid_stat_NCUMR-nmsg_000000L_20211002_000000V.stat
grid_stat_NCUMR-nmsg_000000L_20211002_000000V_nbrcnt.txt
grid_stat_NCUMR-nmsg_000000L_20211002_000000V_cnt.txt
grid_stat_NCUMR-nmsg_000000L_20211002_000000V_nbrctc.txt
grid_stat_NCUMR-nmsg_000000L_20211002_000000V_ctc.txt
grid_stat_NCUMR-nmsg_000000L_20211002_000000V_nbrcts.txt
grid_stat_NCUMR-nmsg_000000L_20211002_000000V_cts.txt
grid_stat_NCUMR-nmsg_000000L_20211002_000000V_pairs.nc
grid_stat_NCUMR-nmsg_000000L_20211002_000000V_eclv.tx
grid_stat_NCUMR-nmsg_000000L_20211002_000000V_sal112.txt
grid_stat_NCUMR-nmsg_000000L_20211002_000000V_fho.txt
grid_stat_NCUMR-nmsg_000000L_20211002_000000V_val112.txt
grid_stat_NCUMR-nmsg_000000L_20211002_000000V_grad.txt
grid_stat_NCUMR-nmsg_000000L_20211002_000000V_vcnt.txt

Acknowledgements: Acknowledgements are due to M. Satheesh and A. Sandeep for the lightning observation extraction and initial setup of the codes for the gridded model forecast lightning flash counts. Model Evaluation Tools (MET) was developed at the National Center for Atmospheric Research (NCAR) through grants from the National Science Foundation (NSF), the National Oceanic and Atmospheric Administration (NOAA), the United States Air Force (USAF), and the United States Department of Energy (DOE). NCAR is sponsored by the United States National Science Foundation.

References

Arakawa, A. and Lamb, V. R., 1977, Computational design of the basic dynamic processes of the UCLA general circulation model, *Methods Comput. Phys.*, 17, 173–265.

Bellouin N, Boucher O, Haywood J, Reddy MS ,2005, Global estimate of aerosol direct radiative forcing from satellite measurements. *Nature*, 438, 1138– 1141, doi:10.1038/nature04348

Best, M. J., et al., 2011, The Joint UK Land Environment Simulator (JULES), model description –Part 1: Energy and water fluxes, *Geosci. Model Dev.*, 4, 677–699, doi:10.5194/gmd-4-677-2011.

Boutle I A, Abel S J, Hill P G and Morcrette C J, 2014, Spatial variability of liquid cloud and rain: observations and microphysical effects; *Q. J. R. Meteorol. Soc.* 140 583–594, <https://doi.org/10.1002/qj.2140>.

Bush, M., Allen, T., Bain, C., Boutle, I., Edwards, J., Finnenkoetter, A., Franklin, C., Hanley, K., Lean, H., Lock, A., Manners, J., Mittermaier, M., Morcrette, C., North, R., Petch, J., Short, C., Vosper, S., Walters, D., Webster, S., Weeks, M., Wilkinson, J., Wood, N. and Zerroukat, M. , 2020, The first Met Office Unified Model–JULES Regional Atmosphere and Land configuration, RAL1. *Geoscientific Model Development*, 13, 1999–2029, <https://doi.org/10.5194/gmd-13-1999-2020>.

Charney, J.G., and N.A.. Philips ,1953, Numerical integration of the Quasi-geostrophic equations for barotropic and simple baroclinic flows, *Journal of Meteorology* , 10(20), 71-99.

Dahl, J. M. L., Höller, H., and Schumann, U., 2011, Modelling the flash rate of thunderstorms. Part I: Framework, *Mon. Wea. Rev.*, 139: 3093–3111, doi: [10.1175/MWR-D-10-05031.1](https://doi.org/10.1175/MWR-D-10-05031.1).

Deierling, W., Petersen, W. A., Latham, J., Ellis, S., Christian, H., The relationship between lightning activity and ice fluxes in thunderstorms, *J. Geophys. Res. (Atmos.)*, 2008, 113(D15210): 1–20, doi: 10.1029/2007JD009700.

Edwards, J. M. and Slingo, A., 1996, Studies with a flexible new radiation code. I: Choosing a configuration for a large-scale model, *Q. J. Roy. Meteor. Soc.*, 122, 689–719, <https://doi.org/10.1002/qj.49712253107>.

Fierro, A. O., Mansell, E. R., MacGorman, D. R., and Ziegler, C. L., 2013, The implementation of an explicit charging and discharge lightning scheme within the WRF-ARW model: Benchmark simulations of a continental squall line, a tropical cycle, and a winter storm. *Mon. Wea. Rev.*, 141: 2390–2415, doi: [10.1175/MWR-D-12-00278.1](https://doi.org/10.1175/MWR-D-12-00278.1).

Fowler, T., J. Halley Gotway, K. Newman, T. Jensen, Brown, B., and R. Bullock, 2017, The Model Evaluation Tools v7.0 (METv7.0) User's Guide. Developmental Testbed Center. Available at: http://www.dtcenter.org/met/users/docs/users_guide/MET_Users_Guide_v7.0.pdf. 407 pp.

Gungle, B., and Krider, E. P., 2006, Cloud-to-ground lightning and surface rainfall in warm-season Florida thunderstorms, *J. Geophys. Res.*, 111(D19203): 1–15, doi: 10.1029/2005JD006802.

Haklander, A. J., and Van Delden, A., 2003, Thunderstorm predictors and their forecast skill for the Netherlands, *Atmos. Res.*, 67–68: 273–299, doi: [10.1016/S0169-8095\(03\)00056-5](https://doi.org/10.1016/S0169-8095(03)00056-5).

Jayakumar A., S. J. Abel, A. G. Turner, S. Mohandas, J. Sethunadh, D. O'Sullivan and E. N. Rajagopal, 2020, Performance of the NCMRWF convection-permitting model during contrasting monsoon phases of 2016 INCOMPASS field campaign. *Quarterly Journal of the Royal Meteorological Society*, DOI:10.1002/qj.3689.

Jayakumar, A., Saji Mohandas, John P George, Devajyoti Duttta, Ashish Routray, Kiran Prasad, Abhijit Sarkar, A.K. Mitra, 2021, NCUM Regional Model Version 4 (NCUM-R: V4), NCMRWF Technical Report NMRF/TR/03/2021, March 2021, National Centre for Medium Range Weather Forecasting, Earth System Science Organisation, Ministry of Earth Sciences , 'Indradhanush', A-50, Sector 62, NOIDA-201 309, India, 27pp.

Kumar, S., M. T. Bushair, Buddhi Prakash J., Abhishek Lodh, Priti Sharma, Gibies George, S. Indira Rani, John P. George, A. Jayakumar, Saji Mohandas, Sushant Kumar, Kuldeep Sharma, S. Karunasagar, and E. N. Rajagopal, 2020, NCUM Global NWP System: Version 6 (NCUM-G:V6), NCMRWF Technical Report NMRWF/TR/06/2020, July 2020, National Centre for Medium Range Weather Forecasting, Ministry of Earth Sciences , Govt. of India, A-50, Sector 62, NOIDA-201 309, India, 32pp.

Kunz, M., 2007, The skill of convective parameters and indices to predict isolated and severe thunderstorms, *Nat. Hazards Earth Syst. Sci.*, 7: 327–342, doi: 10.5194/nhess-7-327-2007.

Lock, AP., 2000, Brown AR, Bush MR, Martin GM, Smith RNB 2000.A New Boundary Layer Mixing Scheme. Part I: Scheme Description and Single-Column Model Tests. *Monthly Weather Review* 128: 3187–3199, DOI:10.1175/1520-0493(2000)128<3187:ANBLMS>2.0.CO;2.

Lott, F. and Miller, M. J., 1977, A new subgrid-scale orographic drag parametrization: Its formulation and testing, *Q. J. Roy. Meteorol. Soc.*, 123, 101–127, <https://doi.org/10.1002/qj.49712353704>.

Lynn, B. H., Yair, Y., Price, C., Kelman, G., and Clark, A. J., 2012, Predicting cloud-to-ground and intracloud lightning in weather forecast models. *Wea. Forecasting*, 27: 1470–1488, doi: [10.1175/WAF-D-11-00144.1](https://doi.org/10.1175/WAF-D-11-00144.1).

McCaul, E. W., Goodman, S. J., LaCasse, K. M., and Cecil, D. J., 2009, Lightning threat using cloud-resolving model simulations, *Wea. Forecasting*, 24: 709–729, doi: [10.1175/2008WAF2222152.1](https://doi.org/10.1175/2008WAF2222152.1).

Mohan, G.M., K. Gayatri Vani, Anupam Hazra, Chandrima Mallick, Hemantkumar S. Chaudhari, Samir Pokhrel, S.D. Pawar, Mahen Konwar, Subodh K. Saha, Subrata K. Das, Sachin Deshpande, Sachin Ghude, M.C. Barth, S.A. Rao, R.S. Nanjundiah, M. Rajeevan, 2021, Evaluating different lightning parameterization schemes to simulate lightning flash counts over Maharashtra, India, *Atmospheric Research*, 255,105532, ISSN 0169-8095, <https://doi.org/10.1016/j.atmosres.2021.105532>.

Price, C., and Rind, D., 1994: Modeling global lightning distributions in a general circulation model, *Mon. Weather Rev* , 122, 1930-1939. [https://doi.org/10.1175/1520-0493\(1994\)1222.0.CO;2](https://doi.org/10.1175/1520-0493(1994)1222.0.CO;2).

Sandeep, A. Jayakumar, M. Sateesh, Saji Mohandas, V. S. Prasad and E. N. Rajagopal, 2021, Assessment of the Efficacy of Lightning Forecast Over India: A Diagnostic Study. *Pure Appl. Geophys.* 178, 205–222. <https://doi.org/10.1007/s00024-020-02627-5>.

Smith, R.N.B. , 1990, A scheme for predicting layer clouds and their water content in a general circulation model. *Quarterly Journal of the Royal Meteorological Society*, 116(492), 435–460.

Vujović, D., Paskota, M., Todorović, N., and Vucković, V., 2015, Evaluation of the stability indices for the thunderstorm forecasting in the region of Belgrade, Serbia. *Atmos. Res.*, 161–162: 143–152, doi: [10.1016/j.atmosres.2015.04.005](https://doi.org/10.1016/j.atmosres.2015.04.005).

Walters, D., Baran, A. J., Boutle, I., Brooks, M., Earnshaw, P., Edwards, J., Furtado, K., Hill, P., Lock, A., Manners, J., Morcrette, C., Mulcahy, J., Sanchez, C., Smith, C., Stratton, R., Tennant, W., Tomassini, L., Van Weverberg, K., Vosper, S., Willett, M., Browse, J., Bushell,

A., Carslaw, K., Dalvi, M., Essery, R., Gedney, N., Hardiman, S., Johnson, B., Johnson, C., Jones, A., Jones, C., Mann, G., Milton, S., Rumbold, H., Sellar, A., Ujiie, M., Whittall, M., Williams, K., and Zerroukat, M., 2019, The Met Office Unified Model Global Atmosphere 7.0/7.1 and JULES Global Land 7.0 configurations, *Geosci. Model Dev.*, 12, 1909–1963, <https://doi.org/10.5194/gmd-12-1909-2019>.

Wilson, D. R. and Ballard, S. P. 1999. A microphysically based precipitation scheme for the UK meteorological office unified model, *Quarterly Journal of the Royal Meteorological Society* 125: 1607–1636. doi:10.1002/qj.49712555707.

Wilson, D.R., Bushell, A.C., Kerr-Munslow, A.M., Price, J.D. and Morcrette, C.J. , 2008, PC2: a prognostic cloud fraction and condensation scheme. I: Scheme description. *Quarterly Journal of the Royal Meteorological Society*, 134(637), 2093– 2107. <https://doi.org/10.1002/qj.333>.

Wood, N., Staniforth, A., White, A., Allen, T., Diamantakis, M., Gross, M., Melvin, T., Smith, C., Vosper, S., Zerroukat, M. and Thuburn, J., 2014, An inherently mass-conserving semi-implicit semi-Lagrangian discretization of the deep-atmosphere global non-hydrostatic equations, *Quarterly Journal of the Royal Meteorological Society*, 140: 1505–1520. doi:10.1002/qj.2235.

Yair, Y., Lynn, B., Price, C., Kotroni, V., Lagouvardos, K., Morin, E., Mugnai, A., and delCarmen Llasat, M., 2010, Predicting the potential for lightning activity in Mediterranean storms based on the weather research and forecasting (WRF) model dynamic and microphysical fields. *J. Geophys. Res.*, 115: D04205, doi: 10.1029/2008JD010868.

Zerroukat, M. and Shipway, B., 2017, ZLF (Zero Lateral Flux): a simple mass conservation method for semi-Lagrangian-based limited-area models, *Q. J. Roy. Meteor. Soc.*, 143, 2578–2584, <https://doi.org/10.1002/qj.3108>.